Crystallization and Shape Evolution of Single Crystalline Selenium Nanorods at Liquid−Liquid Interface: From Monodisperse Amorphous Se Nanospheres toward Se Nanorods

Ji-Ming Song, Jian-Hua Zhu, and Shu-Hong Yu*

Division of Nanomaterials and Chemistry, Hefei National Laboratory for Physical Sciences at Microscale, Structure Research Laboratory of CAS, Department of Chemistry, University of Science and Technology of China, Hefei, Anhui 230026, The People's Republic of China

Received: August 29, 2006; In Final Form: September 24, 2006

The reduction of selenious acid solution with hydrazine hydrate in the presence of poly(vinylpyrrolidone) (PVP) can produce a stable dispersion of uniform and amorphous selenium particles capped with PVP with a size of 100 nm. Further addition of a solvent with low polarity such as *n*-butyl alcohol into this aqueous solution and mild stirring result in the transportation of amorphous selenium particles onto a liquid−liquid interface between water and *n*-butyl alcohol. Subsequent crystallization and shape evolution on this interface occurred and finally resulted in the formation of singe crystalline selenium nanorods. The results demonstrated that the enrichment of nanoparticles with amphiphilic property at a liquid−liquid interface between a polar solvent and another solvent of low polarity can result in crystallization and phase transformation for the formation of nanostructures.

1. Introduction

One-dimensional nanostructures such as nanowires, nanorods, and nanotubes have been the subject of intensive research due to their potential use as active components or interconnects in fabricating nanoscale electronic or electromechanical devices,[1] as well as their important optical, electrical (transport), electrochemical, and mechanical properties.[2] Selenium is well-known for its photoelectrical and semiconductor properties and has been successfully used in solar cells, rectifiers, photographic exposure meters, and xerography.[3] Selenium also has a high reactivity toward a wealth of chemicals that can be potentially exploited to convert into other functional materials such as Ag_2-Se, ZnSe, and CdSe.[4] In addition, selenium is an essential trace element for humans.

Recently, one-dimensional selenium nanoparticles have been fabricated through a few approaches, such as laser ablation,[5] solution-phase approach,[6] vapor-phase growth,[7] electrochemical synthesis,[8] photothermally assisted solution phase,[9] ultrasonic,[10] hydrothermal or solvothermal method,[11] and micelle-mediated synthesis.[12] Ohtani et al. reported a phase conversion from amorphous Se into different polymorphs of Se by exposing amorphous Se with different organic fluids.[13] Designing new approaches to synthesize low-dimensional Se nanostructures under mild conditions is quite important from the viewpoint of fundamental issues and application.

Previously, two-phase heterogeneous solution media have been developed for the synthesis of noble metal nanoparticles[14] and CdS nanoparticles.[15] The oil/water interface has a lot of particular properties that homogeneous solutions do not have. These properties have been widely employed in many fields, such as material synthesis,[16,17] colloid science,[18] and biomimetic domain.[19−21]

In this paper, we demonstrate a facile approach for controlled growth of trigonal Se nanorods, in which addition of *n*-butyl alcohol into an aqueous solution of monodisperse amorphous Se nanospheres stabilized by poly(vinylpyrrolidone) (PVP) results in the transportation of these amphiphilic amorphous Se particles onto a liquid−liquid interface formed between water and *n*-butyl alcohol, and then undergoes further crystallization and phase transformation to form trigonal selenium (t-Se) crystalline nanorods.

2. Experimental Section

2.1. Chemicals. All chemicals are analytical grade, are commercially available from Shanghai Chemical Reagent Co. Ltd., and used in this study without further purification. Poly(vinylpyrrolidone) (PVP, polymerization degree 360) was purchased from Sinopharm Chemical Reagent Co. Ltd.

2.2. Synthetic Procedures. *Synthesis of Amorphous Se Monodisperse Nanoparticles.* In a typical procedure, 5 mL of 0.1 M selenious acid and 5 mL of 0.5 M hydrazine hydrate were put into 10 mL of 0.5% PVP (wt %) at room temperature in turn to form a clear solution, which was then stirred strongly for about 30 min. After that, the solution was kept static. Half an hour later, the mixture slowly changed from yellowish to reddish; the color gradually deepened and finally became cardinal red. Such a color change process usually took about 6−12 h. The final solution was a dispersion of amorphous Se, red in color.

Crystallization of Trigonal Selenium (t-Se) Crystalline Nanorods. In the next step, 10 mL *n*-butyl alcohol was added to the previous mixture solution without separation, after agitating for 10 min, and then the mixture solution was stayed again without stirring. At one time, water and *n*-butyl alcohol from the solution separated quickly because they are not mutually soluble, and an oil/water interface formed immediately. The total solution was divided into three phases. The top layer was *n*-butyl alcohol,

* To whom correspondence should be addressed. Fax: + 86 551 3603040. E-mail: shyu@ustc.edu.cn.

10.1021/jp065600k CCC: $33.50
Published on Web 11/04/2006

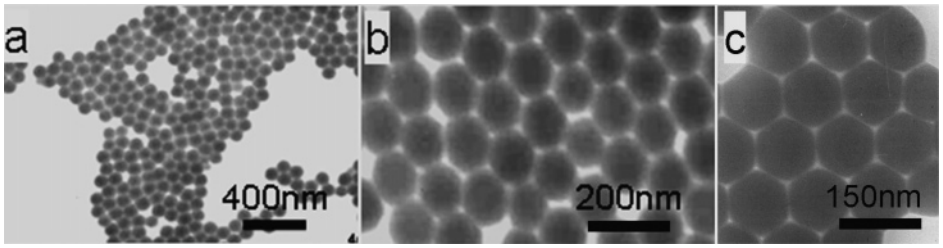

Figure 1. TEM images of obtained selenium sample prepared with homogeneous nucleation process. A 5 mL volume of 0.1 M selenious acid and 5 mL of 0.5 M hydrazine hydrate were put into 10 mL of 0.5% PVP (wt %) at room temperature in turn, to form a clear solution, which was then stirred strongly and kept static for about 30 min, respectively.

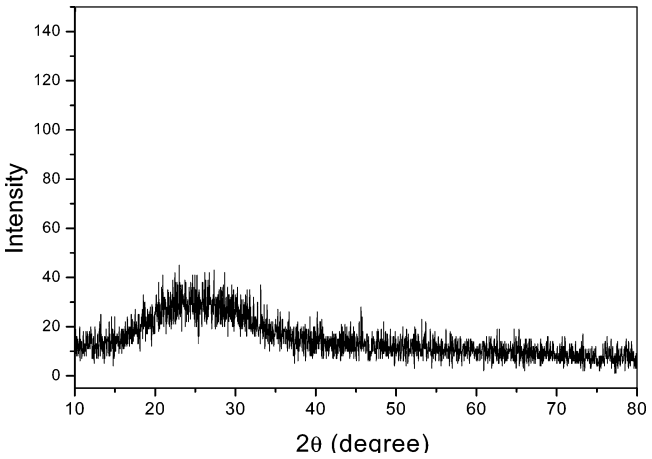

Figure 2. X-ray diffraction (XRD) of the product of amorphous Se.

the bottom layer was water, and the middle layer was an interface comprising amphiphilic molecules and their stabilized amorphous Se particles. The bottom layer and the top layer were clear solution, while all selenium nanoparticles congregated and enriched on the interface. In the beginning, the color of the interface was brick-red and went with a certain metallic shine, subsequently changing rapidly from red to a dust color. This process indicated that the phase transformation occurred to convert from the amorphous Se to the trigonal phase. The products from the interface at different time intervals were taken out and centrifuged and washed several times with double-distilled water (instead of absolute ethanol) for further characterization.

2.3. Characterization. The obtained sample was characterized on an (Philips X'Pert Pro Super) X-ray powder diffractometer with Cu Kα radiation ($\lambda = 1.541\,874$ Å). The morphology was examined by scanning electron microscopy (SEM) analysis on a KYKY-1010B microscope and a field emission SEM microscope (JSM-6700F), by transmission electron microscopy (TEM) performed on a Hitachi (Tokyo, Japan) H-800 transmission electron microscope (TEM) at an accelerating voltage of 200 kV, and by a high-resolution transmission electron microscope (HRTEM) (JEOL-2010) operated at an acceleration voltage of 200 kV. The X-ray photoelectron spectra (XPS) were taken on an ESCALab MKII X-ray photoelectron spectrometer, using Mg Kα radiation as the exciting source. The Raman spectra were performed with 488-nm laser excitation with a micro-Raman system, which was modified by coupling an Olympus microscope to a Spex 1740 spectrometer with a CCD detector. UV−vis spectra were recorded on a UV-2501PC/2550 at room temperature (Shimadzu Corporation, Japan). Fourier transform infrared (FTIR) spectra were measured on a Bruker vector-22 FTIR spectrometer at room temperature.

3. Results and Discussion

3.1. Synthesis of Monodisperse Spherical Colloids of Amorphous Selenium. In recent years, monodisperse spherical colloids have been extensively exploited as the building blocks for self-assembly to generate low-dimensional materials. A number of methods have been demonstrated for generating nanometer-sized particles of amorphous selenium (a-Se), with examples including exposure of selenious acid to γ-radiation[22] and chemical reduction of selenious acid by various reagents,[23] as well as electrochemical oxidation of selenide ion.[24] All of these methods used water as a medium; however, they are only able to prepare samples with a large size distribution. Xia and his colleagues[4] synthesized a-Se spherical colloids with a size distribution difference less than 5% by adopting a more viscous solvent (ethylene glycol) as the reaction medium in place of water. In the present case, the major reaction involved was the reduction of selenious acid in aqueous solution with excess hydrazine at room temperature to generate amorphous selenium (a-Se), nitrogen gas, and water in the presence of poly(vinylpyrrolidone) (PVP). A homogeneous dispersion of brick-red opaque color was obtained.

X-ray diffraction (XRD) shows that the product was amorphous as shown in Figure 2. TEM images in Figure 1 show

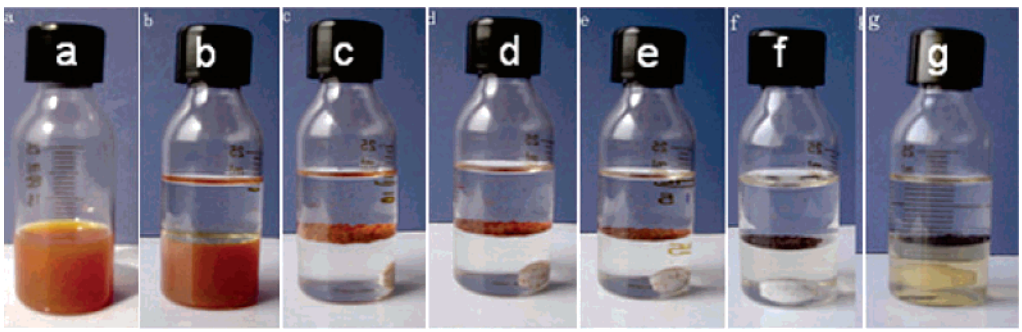

Figure 3. Pictures of several typical stages for the crystallization of selenium nanorods from a-Se to t-Se on the liquid−liquid interface between water and *n*-butyl alcohol. (a) Initial homogeneous dispersion of amorphous Se solution; (b) adding *n*-butyl alcohol without agitating; (c) after agitating for 10 min and stayed for aging; (d) aging for 30 min; (e) aging for 1 h; (f) aging for 2 h; (g) aging for 12 h.

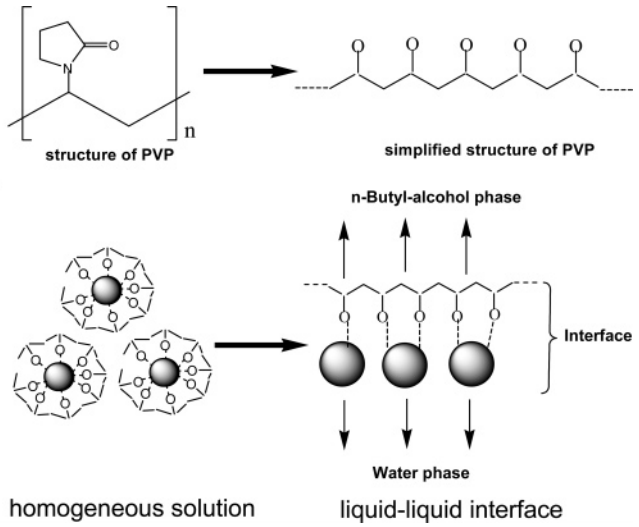

Figure 4. Schematic illustration of the formation mechanism for the transportation of PVP-stabilized amphiphilic a-Se particles onto a liquid−liquid interface formed between water and *n*-butyl alcohol, which then undergoes further crystallization and phase transformation for the formation of trigonal selenium (t-Se) crystalline nanorods.

that the particles are homogeneous with an average size of 100 ± 5 nm, which is much smaller than those reported previously by refluxing method.[25] These colloidal nanoparticles were stable in aqueous solution even after several weeks of storage. The results showed that these amorphous particles did not tend to grow or crystallize further.

3.2. Crystallization and Formation of One-Dimensional Selenium Nanorods on Liquid−Liquid Interface. With the addition of *n*-butyl alcohol into the above dispersion, an interface formed immediately (Figure 3a,b); with the help of stirring all a-Se particles were transported onto the liquid−liquid interface between water and *n*-butyl alcohol (Figure 3c). With aging time prolonged up to 2 h, the color changed to black-gray, indicating that the phase transformation happened on that interface (Figure 3d−f). After aging for 12 h, black solid aggregates formed on that interface (Figure 3g). The phase transportation process can be schematically illustrated as in Figure 4, where the PVP-stabilized a-Se particles are amphiphilic and will be transported onto that interface.

Figure 5a shows the XRD pattern of the sample prepared via interface growth for 12 h, which confirms the formation of crystalline selenium. All the diffraction peaks in this pattern can be indexed as a hexagonal phase of selenium (JCPDS, No. 6-362) with a cell constant and $a = 4.37$ Å, $c = 4.95$ Å. The (100) diffraction peak is unusually stronger than the (101) diffraction peak, indicating the possible preferential orientation of the Se nanostructures. The differential scanning calorimetric (DSC) curve of the crystallized Se product exhibits an endothermic peak at 217.9 °C (Figure 5b), which is close to the melting point of bulk trigonal selenium (217 °C) but far from that of monoclinic Se (∼175 °C) and a-Se (∼70 °C). Apparently, this result supports that the product is indeed made of t-Se.

TEM images in Figure 6 show that the product is composed of nanorods with diameters of 100−120 nm and lengths up to several tens of micrometers. Selected area electron diffraction pattern (SAED) showed that the nanorods are single crystalline (inset in Figure 6a). Some of the nanorods are straight and some of them are bent (Figure 6b,c). The high-resolution electron microscopy (HRTEM) images in Figure 7c,d were taken from the edge and tip of the single crystalline nanorod shown in Figure 7a, showing lattice spacings of ca. 5.0 and 3.8 Å, respectively, corresponding to the lattice spacings of the (001) and (100) planes for trigonal selenium. Figure 7b shows the corresponding electron diffraction pattern of the single nanorod, which was obtained by focusing the electron beam along the [010] axis. Both HRTEM and SAED patterns confirmed that the axis of the nanorod is along the [001] direction.

Figure 8a shows the XPS analysis. The strong peak at 54.9 eV correspond to Se 3d binding energy. No peaks for selenium oxide or other impurity peaks are observed, indicating high purity of the product. At the same time, no peak for N 1s of PVP at 399 eV was detected on the XPS survey spectrum, underlying that there is no residual PVP on the surfaces of Se nanorods after the samples have been washed several times. This is different from the interaction between Ag atoms and PVP molecules as reported previously.[26] The Raman spectrum in Figure 8b shows a resonance peak at 234.8 cm^{-1} which is a characteristic stretching mode of a chainlike structure that only exists in trigonal selenium, and is assigned to the A1 mode.[10b] The resonance peak of one E mode is also at about 234 cm^{-1}, which may be overlapped by the strong peak of A1. The peaks at 436.6 and 460.3 cm^{-1} can be attributed to the second-order spectra of trigonal selenium.[27] Raman peaks for monoclinic selenium and a-Se at ∼256 and ∼264 cm^{-1} are not observed in Figure 8b. These results indicate that trigonal selenium of high purity was produced by this approach.

3.3. Growth Mechanism of Selenium Nanostructures. It is well-known that trigonal Se is the most stable phase of all Se allotropes.[7a] Previously, amorphous selenium particles could

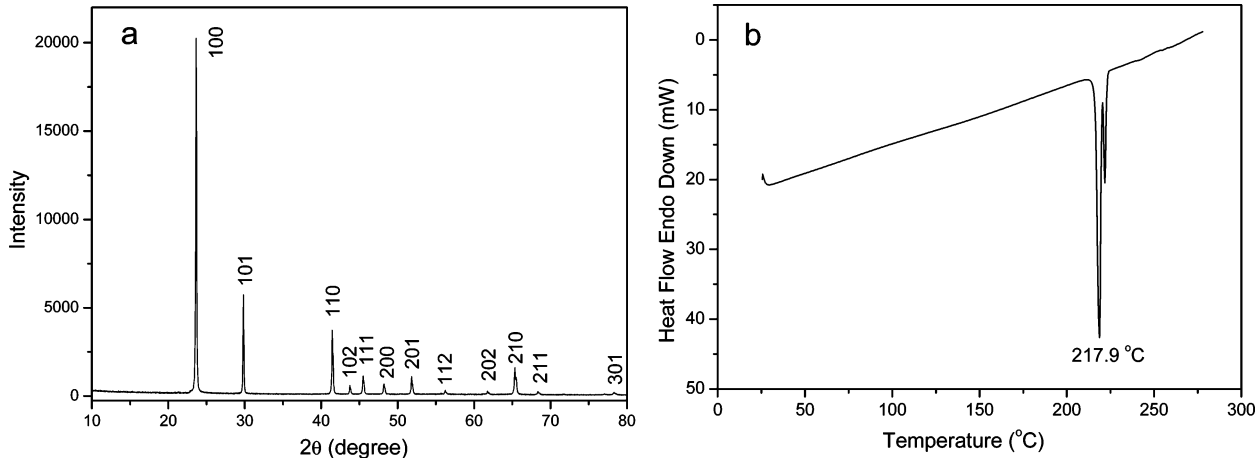

Figure 5. (a) XRD pattern of the product formed on the liquid−liquid interface after aging for 12 h. (b) DSC curve of as-prepared product.

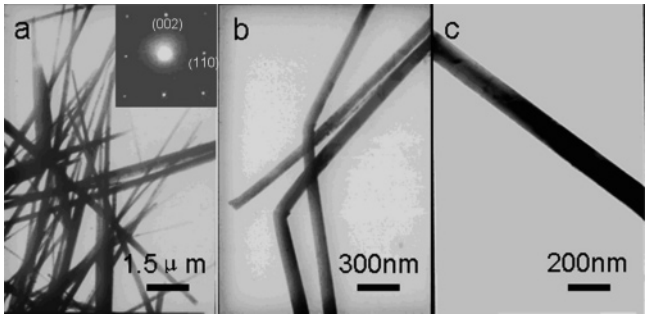

Figure 6. (a) TEM images of selenium nanorods obtained at liquid−liquid interface. (b)−(c) Enlarged TEM images. Inset shows a typical electron diffraction pattern of Se nanorods.

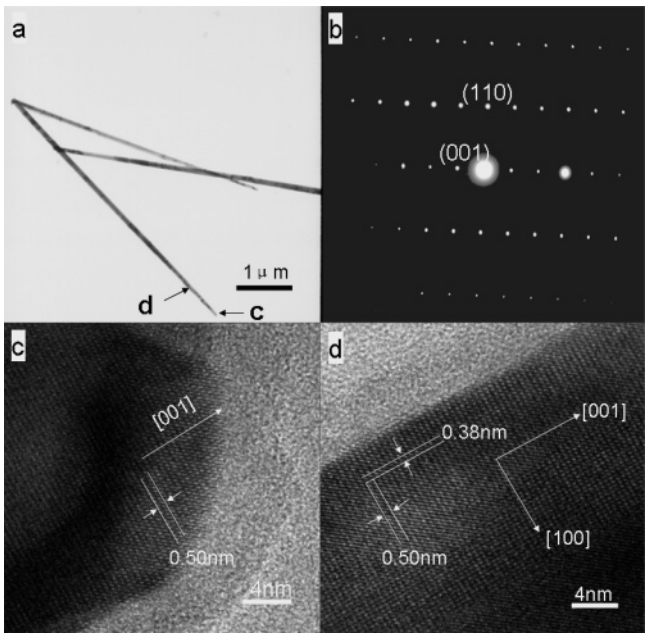

Figure 7. (a) TEM image of Se nanorods. (b) SAED pattern taken along [010] direction. (c, d) HRTEM images of different areas (indicated in (a)) of an individual rod. The HRTEM images show lattice spacings of 5.0 and 3.8 Å are observed. Fringes with a spacing of 0.50 nm are observed, which are perpendicular to the axial direction, indicating that the nanorod grew along [001].

be dissolved and transformed into trigonal phase slowly under certain conditions.[3] To examine the detailed phase transformation, crystallization, and shape evolution processes in the present system, the intermediate products obtained after different time intervals were taken for further analysis. The growth process is involved in both the linear aggregation of a-Se spheres and crystallization from the amorphous phase. Even though the previous report has shown that a-Se can be transformed into t-Se under illumination of light,[28] a-Se particles are stable in the present case without addition of *n*-butyl alcohol. This implies that the transportation of a-Se onto the liquid−liquid interface and the following contact with *n*-butyl alcohol solvent played crucial roles in the following phase transformation and crystallization process, which is consistent with the previous observation of the crystallization of different phases of Se compound from a-Se in different organic fluids.[13]

UV−vis spectra and XRD patterns were used to follow the crystallization process and accompanying color changes for the intermediate products at different time intervals. From the UV−vis absorbance spectra, the red shift and the broadening of the absorption peak are very apparent along with prolonged aging time (Figure 9, left), indicating that the growth in size of the colloid particles has the same trend as the spectroscopic measurements by Tarcha et al.,[29] but the opposite trend found in a refluxing process for synthesis of t-Se by rupturing of a-Se colloidal particles for seeding growth of t-Se.[3] The intensity change and the position shift (red shift) of the absorbance peaks might be associated with the length variation of the rods and crystallization behaviors of one-dimensional nanostructures. It was reported that the optical property of Se could be adjusted by changing the synthetic conditions and, thus, the size and microstructure of the formed Se nanomaterials.[30] The corresponding XRD patterns for the products obtained after different time intervals suggested that a-Se directly transformed into stable t-Se without going through a metastable monoclinic Se phase (Figure 9, right). The diffraction intensity of the (101) face is stronger than that of the (100) face before aging for 30 min; however, the relative intensity of (100) will prevail over that of (101) with aging time prolonged further. This is another indication of the phase transformation, crystallization, and preferential growth during the aging period.

Time-dependent shape evolution of t-Se nanorods has been examined also. Figure 10a,b indicates that the amorphous Se spheres tend to aggregate to form linear aggregates after aging for 10 min. With prolonging time, the particles start crystallization spontaneously without addition of foreign t-Se seeds as reported previously,[3] but it is similar to that found previously after exposing amorphous Se with a organic solvent.[13] Accompanying the crystallization, the amorphous Se particles tend to aggregate and dissolve partially as a result of Rayleigh

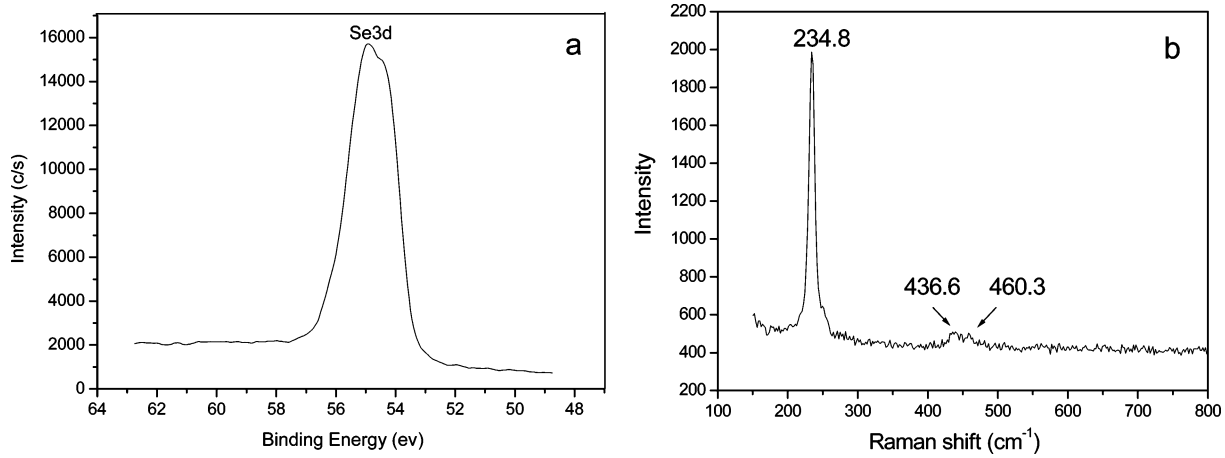

Figure 8. (a) XPS survey of Te 3d region. (b) Raman scattering spectrum of the Se nanorods. The resonance peak at 234.8 cm^{-1} is a characteristic stretching mode of t-Se.

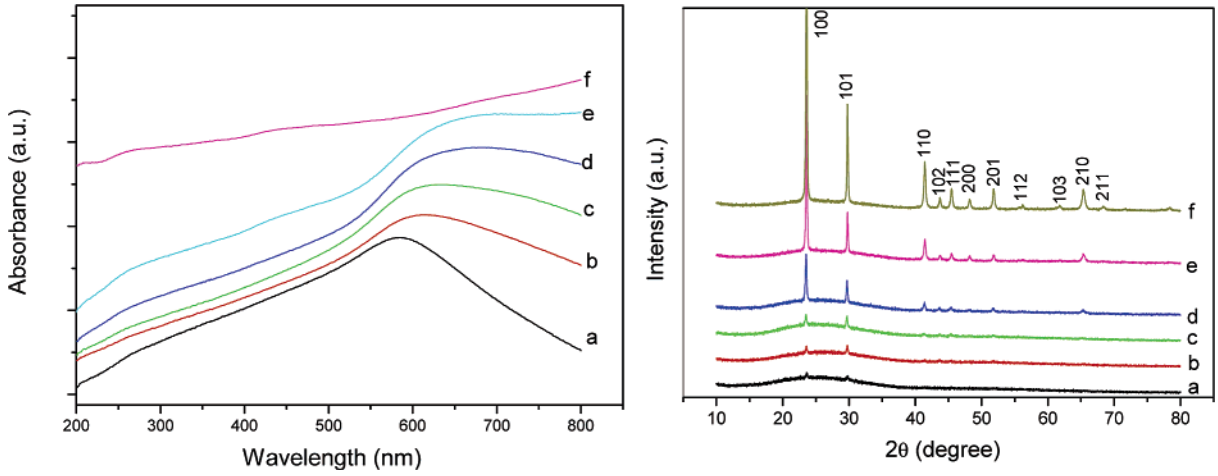

Figure 9. (left) Time-dependent UV−vis absorbance spectra for the samples taken at different time intervals. The samples were immediately taken out and redispersed in water for UV−vis measurement. (right) Time-dependent XRD patterns recorded for the samples obtained at different time intervals: (a) aging for 10 min; (b) aging for 20 min; (c) aging for 30 min; (d) aging for 1 h; (e) aging for 3 h; (f) aging for 12 h.

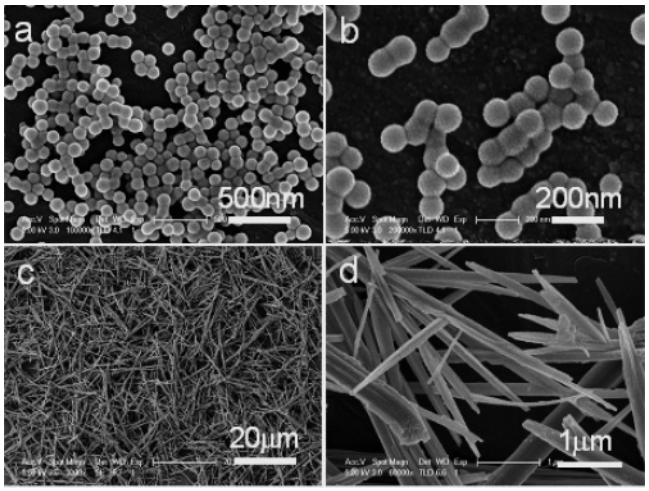

Figure 10. SEM images of selenium samples prepared by aging of monodisperse spherical colloids of amorphous selenium after different aging time: (a, b) aging for 10 min; (c, d) aging for 12 h.

instability[31] with the same trend as previously reported by Xia et al.[3] The ripened t-Se nanorods will form finally after undergoing the Ostwald ripening process (Figure 10c,d and Figure 11), where the ripening rods grew at the cost of the smaller aggregated nanoparticles.

PVP, as a polymer surfactant, has been proven to play an important role in the synthesis of one-dimensional nanorods and nanowires of selenium. In fact, the effects of PVP on the synthesis of selenium nanostructures are rather complicated. In the present experiment, *n*-butyl alcohol was selected as the oil phase, for the density of *n*-butyl alcohol is smaller than that of pure water and its solubility is only 8% (wt %) in pure water at room temperature. PVP molecule chains wind around Se nanospheres for sorption before the interface has been formed. These molecule chains are rearranged after *n*-butyl alcohol has been added to the Se colloidal dispersion due to their amphiphilic property. At the liquid−liquid interface such amphiphilic molecules orient themselves with their hydrocarbon chains upward in the low polar alcohol phase and their hydrophilic headgroups downward into the high polar aqueous phase (Figure 4). Thus, at least an interfacial monolayer formed which will confine and induce growth of crystalline Se nanoparticles. The a-Se colloid particles could rapidly aggregate at the interface; there are two possible reasons: First, concentration of the particles was greatly augmented as all particles were transported toward the thin interface. Second, the interaction forces of particles with ambient were already changed due to

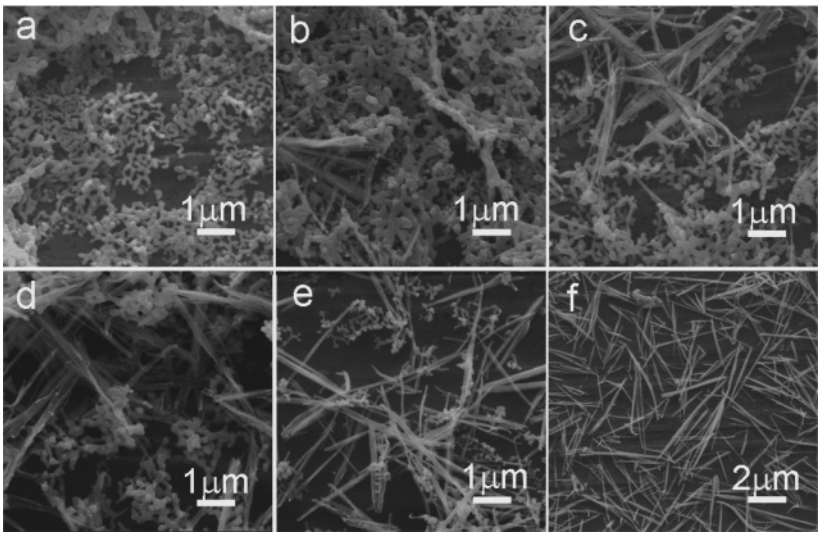

Figure 11. SEM images of selenium samples prepared by aging of monodisperse spherical colloids of amorphous selenium after different aging time: (a) after agitating for 10 min; (b) aging for 20 min; (c) aging for 30 min; (d) aging for 1 h; (e) aging for 2 h; (f) aging for 12 h.

exposing their surface to *n*-butyl alcohol. Colloidal particles in this solution are subject to attractive forces, but these forces are equal in the bulk of the solution. However, at an interface the forces are unequal and the net effect is to pull the peripheral particles into the bulk of the solution (up or down). The particles at the interface are subject to gravity, pressure of above the liquid column and the atmosphere, buoyancy, interfacial tensile force from both oil and water, and even dispersion force owing to the short distance of vicinity particles. The interaction of all these forces can keep these Se nanoparticles at the interface and then undergo the crystallization process.

Other solvents of low polarity or nonpolarity, such as acetone, benzene, carbon tetrachloride, *n*-hexane, and ethyl ether, were also used instead of *n*-butyl alcohol in the present system. The results showed that there was no interface formed in the case of acetone because it is mutually soluble with aqueous solution. While the liquid−liquid interface will form for other solvents such as benzene, carbon tetrachloride, *n*-hexane, and ethyl ether, selenium nanoparticles cannot be drawn onto the liquid−liquid interface but still stay in the water phase, and thus do not undergo crystallization and shape evolution as in the case of *n*-butyl alcohol. However, isopentyl alcohol and other alcohols of low polarity can have an influence similar to that of *n*-butyl alcohol on the crystallization and shape evolution of amorphous selenium nanospheres.

4. Conclusions

In summary, chemical reduction of selenious acid solution with hydrazine hydrate in the presence of poly(vinylpyrrolidone) (PVP) can produce a stable dispersion of monodisperse amorphous selenium nanoparticles capped with PVP and a size of 100 nm. These amorphous Se nanospheres with amphiphilic property can be transported to a liquid−liquid interface formed by adding a solvent with low polarity such as *n*-butyl alcohol into such a dispersion. Those amorphous Se spheres have been found to undergo crystallization and shape evolution into single crystalline Se nanorods. The results demonstrated an example that the enrichment of nanoparticles with amphiphilic property onto a liquid−liquid interface between a polar solvent and another solvent of low polarity can result in crystallization and phase transformation for the formation of nanostructures. This method is expected for the controlled synthesis of other nanostructures at a liquid−liquid interface.

Acknowledgment. We thank the Centurial Program of the Chinese Academy of Sciences, the National Science Foundation of China (Nos. 20325104, 20321101, 50372065), and the Scientific Research Foundation for the Returned Overseas Chinese Scholars supported by the State Education Ministry, the Specialized Research Fund for the Doctoral Program (SRFDP) of Higher Education State Education Ministry, and the Partner-Group of the Chinese Academy of Sciences−The Max Planck Society.

References and Notes

(1) (a) Duan, X.; Huang, Y.; Cui, Y.; Wang, J.; Lieber, C. M. *Nature (London)* **2001**, *409*, 66. (b) Huang, H. M.; Mao, S.; Feick, H.; Yan, H.; Wu, Y.; Kind, H.; Weber, E.; Russo, R.; Yang, P. *Science* **2001**, *292*, 1897. (c) Chung, S. W.; Yu, J. Y.; Heath, J. R. *Appl. Phys. Lett.* **2000**, *76*, 2068.

(2) (a) Hu, J.; Odom, T. W.; Lieber, C. *Acc. Chem. Res.* **1999**, *32*, 435. (b) Prokes, S. M.; Wang, K. L. *MRS Bull.* **1999**, *24*, 13. (c) Wang, Z. L. *Adv. Mater.* **2000**, *12*, 1295. (d) Mayers, B.; Gates, B.; Yin, Y. D.; Xia, Y. N. *Adv. Mater.* **2001**, *13*, 1380.

(3) Gates, B.; Mayers, B.; Cattle, B.; Xia, Y. N. *Adv. Funct. Mater.* **2002**, *12*, 219.

(4) (a) Gates, B.; Wu, Y. Y.; Yin, Y. D.; Yang, P. D.; Xia, Y. N. *J. Am. Chem. Soc.* **2001**, *123*, 11500. (b) Henshaw, G.; Parkin, I. P.; Shaw, G. A. *J. Chem. Soc., Dalton Trans.* **1997**, *231*, 6.

(5) Jiang, Z. Y.; Xie, Z. X.; Xie, S. Y.; Zhang, X. H.; Huang, R. B.; Zheng, L. S. *Chem. Phys. Lett.* **2003**, *368*, 425.

(6) (a) Gates, B., Yin, Y. D.; Xia, Y. N. *J. Am. Chem. Soc.* **2000**, *122*, 12582. (b) Zhang, H.; Yang, D.; Ji, Y. J.; Ma, X. Y.; Xu, J.; Que, D. L. *J. Phys. Chem. B* **2004**, *108*, 1179.

(7) (a) Cao, X. B.; Xie, Y.; Zhang, S. Y.; Li, F. Q. *Adv. Mater.* **2004**, *16*, 649. (b) Ren, L.; Zhang, H. Z.; Tan, P. H.; Chen, Y. F.; Zhang, Z. S.; Chang, Y. Q.; Xu, J.; Yang, F. H.; Yu, D. P. *J. Phys. Chem. B* **2004**, *108*, 4627.

(8) Zhang, S. Y.; Liu, Y.; Ma, X.; Chen, H. Y. *J. Phys. Chem. B* **2006**, *110*, 9041.

(9) Zhang, B.; Dai, W.; Ye, X. C.; Zuo, F.; Xie, Y. *Angew. Chem., Int. Ed.* **2006**, *45*, 2571.

(10) (a) Mayers, B. T.; Liu, K.; Sunderland, D.; Xia, Y. N. *Chem. Mater.* **2003**, *15*, 3852. (b) Li, X. M.; Li, Y.; Li, S. Q.; Zhou, W. W.; Chu, H. B.; Chen, W.; Li, I.; Tang, Z. K. *Cryst. Growth Des.* **2005**, *5*, 911.

(11) (a) Lu, Q. Y.; Gao, F.; Komarneni. S. *Chem. Mater.* **2006**, *18*, 159. (b) Ding, Y.; Li, Q.; Jia, Y. B.; Chen, L.; Xing, J. Y.; Qian, Y. T. *J. Cryst. Growth* **2002**, *241*, 489.

(12) Ma, Y. R.; Qi, L. M.; Ma, J. M.; Cheng, H. M. *Adv. Mater.* **2004**, *16*, 1023.

(13) Ohtani, T.; Takayama, N.; Ikeda, K.; Araki, M. *Chem. Lett.* **2004**, *33*, 100.

(14) Brust, M.; Walker, M.; Bethell, D.; Schiffrin, D. J.; Whyman, R. *Chem. Commun.* **1994**, *7*, 801.

(15) Pan, D. C.; Jiang, S. C.; An, L. J.; Jiang, B. Z. *Adv. Mater.* **2004**, *16*, 982.

(16) Wang, X.; Zhuang, J.; Peng, Q.; Li, Y. D. *Nature (London)* **2005**, *437*, 121.

(17) (a) Fujiwara, M.; Shiokawa, K.; Tanaka, Y.; Nakahara, Y. *Chem. Mater.* **2004**, *16*, 5420. (b) Talapin, D, V.; Shevchenko, E. V.; Kornowski, A.; Gaponik, N.; Haase, M.; Rogach, A. L.; Weller, H. *Adv. Mater.* **2001**, *13*, 1868.

(18) (a) Velev, O. D.; Furusawa, K.; Nagayama, K. *Langmuir* **1996**, *12*, 2385. (b) Velev, O. D.; Nagayama, K. *Langmuir* **1997**, *13*, 1856.

(19) Fendler, J. H.; Meldrum, F. C. *Adv. Mater.* **1995**, *7*, 607.

(20) Heywood, B. R.; Mann, S. *Langmuir* **1992**, *8*, 1492.

(21) Kuang, D.; Xu, A. W.; Fang, Y. P.; Ou, H. D.; Liu, H. Q. *J. Cryst. Growth* **2002**, *244*, 379.

(22) Zhu, Y.; Qian, Y.; Huang, H.; Zhang, M. *Mater. Lett.* **1996**, *28*, 119.

(23) Smith, T. W.; Cheatham, R. A. *Macromolecules* **1980**, *13*, 1203.

(24) Franklin, T. C.; Adeniyi, W. K.; Nnodimele, R. *J. Electrochem. Soc.* **1990**, *137*, 480.

(25) Watillon, A.; Dauchot, J. *J. Colloid Interface Sci.* **1968**, *27*, 507.

(26) Gao, Y.; Jiang, P.; Liu, D. F.; Yuan, H. J.; Yan, X. Q.; Zhou, Z. P.; Wang, J. X.; Song, L.; Liu, L. F.; Zhou, W. Y.; Wang, C. Y.; Xie, S. S. Zhang, J. M.; Shen, D. Y. *J. Phys. Chem. B* **2004**, *108*, 12877.

(27) Lucovsky, G.; Mooradian, A.; Taylor, W.; Wright, G. B.; Keezer, R. C. *Solid State Commun.* **1967**, *5*, 113.

(28) (a) Dresner, J.; Stringfellow, G. B. *J. Phys. Chem. Solids* **1968**, *29*, 303. (b) Ishida, K.; Tanaka, K. *Phys. Rev. B* **1997**, *56*, 206.

(29) Mees, D. R.; Pysto, W.; Tarcha, P. J. *J. Colloid Interface Sci.* **1995**, *170*, 254.

(30) Chizhikov, D. M.; Shchastlivyi, V. P. *Selenium and Selenides*; Collets Publishing: London, 1968.

(31) Quere, D.; Di Meglio, J.-M.; Brochard-Wyart, F. *Science* **1990**, *249*, 1256.